Adv. Radio Sci., 10, 327–332, 2012
www.adv-radio-sci.net/10/327/2012/
doi:10.5194/ars-10-327-2012

Advances in Radio Science

Differential Algebraic Equations of MOS Circuits and Jump Behavior

P. Sarangapani[1], T. Thiessen[2], and W. Mathis[2]

[1]Indian Institute of Technology, Madras, India
[2]Institute of Theoretical Electrical Engineering, Leibniz University of Hannover, Germany

Correspondence to: T. Thiessen (thiessen@tet.uni-hannover.de)

Abstract. Many nonlinear electronic circuits showing fast switching behavior exhibit jump effects which occurs when the state space of the electronic system contains a fold. This leads to difficulties during the simulation of these systems with standard circuit simulators. A method to overcome these problems is by regularization, where parasitic inductors and capacitors are added at the suitable locations. However, the transient solution will not be reliable if this regularization is not done in accordance with Tikhonov's Theorem. A geometric approach is taken to overcome these problems by explicitly computing the state space and jump points of the circuit. Until now, work has been done in analyzing example circuits exhibiting this behavior for BJT transistors. In this work we apply these methods to MOS circuits (Schmitt trigger, flip flop and multivibrator) and present the numerical results. To analyze the circuits we use the EKV drain current model as equivalent circuit model for the MOS transistors.

1 Introduction

In this work our focus lies on circuits which exhibit fast switching behavior (Schmitt Trigger, flip flop and multivibrator). It is known that the derivative of the capacitor voltages and inductor currents govern the dynamics of an electronic circuit. Also, the differential equations of electronic circuits can be viewed as a flow on the state space manifold, which is represented by the algebraic constraints of the circuit. These circuits with discontinuous changes in states, which are called "jumps in state space", contain a fold in their state space manifold. The simulation of these circuits leads to a simulation failure as the circuit can adopt multiple operating points at the same time. A method to overcome this problem is to regularize the system by adding capacitors and inductors at appropriate nodes, in accordance with Tikhonov's theorem (Tikhonov et al., 1985). When the network is ϵ-regularized (Ihrig, 1975), the jump behavior can be viewed as the limit $\epsilon \to 0$ of the solutions of the singularly perturbed system (Sastry and Desoer, 1981). This method can regularize the system, but it gives erroneous transient solutions by choosing wrongly located L's and C's. Another problem is due to the widely spaced time-constants, which appear because the dynamics of a regularized circuit can be divided into a slow and a fast part, leading to the so-called "time-constant problem" of circuit simulation (Sandberg and Shichman, 1968). Hence, we adopt a geometric approach and calculate the jump points and state space explicitly. This approach has been succesfully applied to example transistor circuits involving BJTs. In this work, we apply the method to MOS circuits and calculate the state space and jump points for Schmitt Trigger, flip flop and multivibrator and show that the results confirm with the simulation results. To efficiently model the MOS circuits, the EKV drain current model has been used (Enz et al., 1995).

2 Geometric interpretation of jump behavior

The state space $\mathcal{S}$ of an electronic circuit can be interpreted as a differentiable manifold and is given by the intersection of the Ohmian $\mathcal{O}$ and the Kirchhoffian $\mathcal{K}$ space $\mathcal{S} := \mathcal{K} \cap \mathcal{O}$ (Smale, 1972; Desoer and Wu, 1972; Chua, 1980). The dynamics of an electronic circuit then is defined on $\mathcal{S}$ (Mathis, 1992). This implies that we need to satisfy the following conditions: (1) $\mathcal{S}$ is a smooth manifold and (2) the dynamics can be created on $\mathcal{S}$. The first is a typical or so-called generic condition (for a detailed discussion, see Mathis, 1992), and

Published by Copernicus Publications on behalf of the URSI Landesausschuss in der Bundesrepublik Deutschland e.V.

in the following we assume $\mathcal{S}$ to be a smooth manifold. The second condition requires the construction of a vector field X on the smooth manifold $\mathcal{S}$. Based on fundamental physical laws, the relationships between currents and voltages of capacitors and inductors are given by means of differential relations. Therefore these differential equations are formulated in i_{L} and u_{C} coordinate planes. Now, one has to "lift" or "pull-back" the dynamics on the state space $\mathcal{S}$. Therefore, the vector field ceases to exist if the pull-back or the dynamics is degenerated, which leads to jumps in $\mathcal{S}$. This degeneracy occurs if $\mathcal{S}$ contains a fold. A detailed discussion of degeneracy can be found in Thiessen and Mathis (2011) and Mathis (1992).

If the circuit is characterized by the following algebro-differential equations (DAEs) in a semi explicit form:

$$\dot{\boldsymbol{x}} = \boldsymbol{g}(\boldsymbol{x}, \boldsymbol{y}, z) \qquad \boldsymbol{g}: \mathbb{R}^k \rightarrow \mathbb{R}^n \tag{1}$$

$$\boldsymbol{0} = \boldsymbol{f}(\boldsymbol{x}, \boldsymbol{y}, z) \qquad \boldsymbol{f}: \mathbb{R}^k \rightarrow \mathbb{R}^m \tag{2}$$

then the set of all jump points (jump-set) is characterized by

$$\mathbf{J} = det\left(\partial_{\boldsymbol{y}} \boldsymbol{f}(\boldsymbol{x}, \boldsymbol{y}, z)\right) = \boldsymbol{0} \text{ where } \boldsymbol{f}(\boldsymbol{x}, \boldsymbol{y}, z) = \boldsymbol{0}. \tag{3}$$

(see also Nielsen and Willson Jr. (1980), Tchizawa (1984), Ichiraku (1979),Thiessen et al. (2012)). The vector $\boldsymbol{x} \in \mathbb{R}^n$ corresponds to the capacitor voltages and inductor currents and $\boldsymbol{y} \in \mathbb{R}^m$ is a vector of additional voltages and currents. Since there are circuits which exhibit a fold respectively their input voltages, we assign an additional vector $\boldsymbol{z} \in \mathbb{R}^\eta$ to independent voltage or current input sources. We treat the independent input sources as norators and assume $\boldsymbol{z}$ to be another variable in our system of equations. Therefore, the state space $\mathcal{S}$ of the circuit has to be extended by the number of independent sources η. Now, the dimension k of the embedding space $\mathcal{E} \in \mathbb{R}^k$ can be determined by $k = n + m + \eta$ and the dimension of $\mathcal{S}$ by $dim(\mathcal{S}) = l = n + \eta$. The state space $\mathcal{S}$ can be defined as a subspace of the $\mathcal{E}$ and is represented by the solution set of the algebraic equations (2). The dynamical beahvior of the circuit is represented by the differential equations (1).

The jump takes place in a subspace parallel to the space spanned by $\boldsymbol{y}$, where $\boldsymbol{y}$ is the vector of all coordinates which are not fixed and do not conserve energy Thiessen and Mathis (2011), Thiessen et al. (2012). The corresponding "hit-set" is the intersection of the "bundle" of all jump spaces at points of the jump-set and the state space $\mathcal{S}$.

To solve the equivalent circuits of the Schmitt Trigger, flip flop and multivibrator, we take this approach where we numerically calculate the jump points. For the determination of $\mathcal{S}$, we interpret $\boldsymbol{z}$ as variables and by specifying l components of $\boldsymbol{y}$, we can calculate $\mathcal{S}$ Thiessen et al. (2012).

3 Modelling the MOS equivalent circuit

It is known that the MOS drain current follows a square law and is a function of the gate-source and the drain-source voltages and goes to zero below V_{th}. It is seen, that below the threshold voltage the current-voltage characteristic is exponential and is called as sub-threshold current and the behavior is as follows

$$I_d = I_{\mathrm{S}} \frac{W}{L} \exp\left(\frac{\kappa V_{\mathrm{gs}}}{U_{\mathrm{T}}}\right)\left[1 - \exp\left(\frac{-V_{\mathrm{ds}}}{U_{\mathrm{T}}}\right)\right], \tag{4}$$

where U_{T} is the thermal voltage, κ the non-ideality factor and I_{S} is the saturation current. Since we are dealing with circuits that are switching from cutoff to saturation, we need a model that holds good for all regions of operation and does not exhibit the jump in the current function itself, as seen in the square law case. Hence, we use the EKV drain current equation, which is valid in all regimes. The following equation shows the EKV current characteristic.

$$I_d = 2\mu_n C_{\mathrm{ox}} \frac{W}{L} U_{\mathrm{T}}^2 \ln^2\left(1 + \exp\left(\frac{V_{\mathrm{gs}} - V_t}{2\kappa U_{\mathrm{T}}}\right)\right), \tag{5}$$

where κ is a variable and is adjusted according to the MOS under consideration. We can see that when V_{gs} is a significant value, the exponent dominates inside the logarithm and hence we can approximate $\ln(1+e^x) \approxeq \ln(e^x) = x$. Upon using this approximation we get

$$I_d = \frac{\mu_n C_{\mathrm{ox}}}{2\kappa^2} \frac{W}{L} \left(V_{\mathrm{gs}} - V_t\right)^2. \tag{6}$$

If the gate source potential is a value comparable or less than V_t, then we can approximate $\ln(1+e^x) \approxeq e^x$. With this approximation we get

$$I_d = 2\mu_n C_{\mathrm{ox}} \frac{W}{L} U_{\mathrm{T}}^2 \exp\left(\frac{V_{\mathrm{gs}} - V_t}{\kappa U_{\mathrm{T}}}\right). \tag{7}$$

Figure 1 illustrates how the EKV equation closely resembles the square law curve as well as the sub-threshold current in their respective regimes. The threshold voltage used for the analysis is $V_{\mathrm{th}} = 1.6\,\mathrm{V}$. We compare the EKV model with the actual MOS (BSS123) that is going to be used for the subsequent analysis. From the parameters of the BSS123 MOS, we calculate the constants that need to be used in the EKV model. It gives us the following empirical drain current equation, which can be used to simulate the circuits.

$$f(v) = a \cdot \ln^2(1 + \exp(b(V_{\mathrm{gs}} - 1.6))), \tag{8}$$

where $a = 0.0013$ and $b = 10.7250$. Figure 2 shows the drain current versus the gate source voltage characteristic of the EKV approximation and the BSS123 for $\kappa = 1.8$.

4 Example 1: Schmitt Trigger circuit

In this section we analyze the Schmitt Trigger circuit from a geometric point of view. The design parameters of the circuit are $R_{\mathrm{c1}} = 2.5\,\mathrm{k\Omega}$, $R_{\mathrm{c2}} = 1\,\mathrm{k\Omega}$, $R_1 = 10\,\mathrm{k\Omega}$, $R_2 = 12\,\mathrm{k\Omega}$,

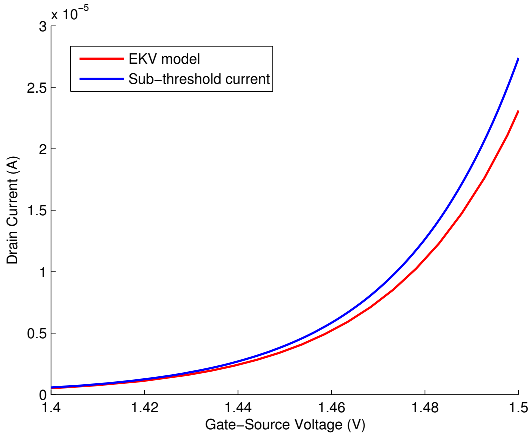

(a) Sub-Threshold Case

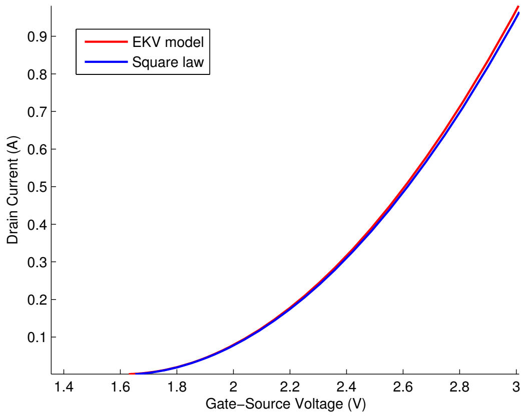

(b) Square-Law Case

Fig. 1. Comparison of the EKV model with the square law and sub-threshold current.

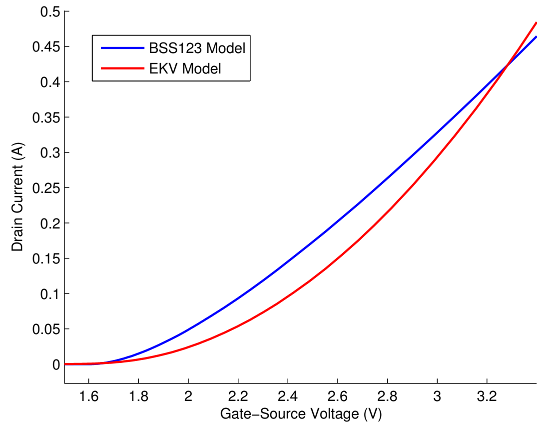

Fig. 2. Comparison of the EKV model with the BSS123 MOS.

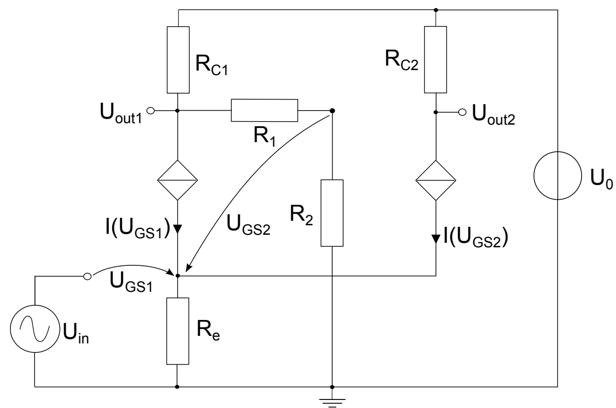

Fig. 3. Schmitt Trigger Circuit.

$R_\mathrm{e} = 300\,\Omega$, $U_\mathrm{o} = 9$ V and $V_\mathrm{T} = 1.6$ V. We neglect the gate source capacitance during the calculation of the jump points. These capacitances are used to regularize the circuit and therefore enable the simulation of the circuits with a common circuit simulator. In our approach, addition of these regularization capacitances C_T is not necessary. Equation (9) gives us the state space description of the system. U_in is the input and U_gs1 and U_gs2 are the gate source voltages and are set as the state variables. $f(.)$ is the EKV equation as described in Eq. (8). The output voltages are then found out as a function of U_gs1, U_gs2. The state space of the circuit is given by the intersection of the solution sets of these two equations:

$$\begin{aligned}0 &= U_\mathrm{in}\left(\frac{1}{R_\mathrm{e}} - k\right) + U_\mathrm{gs1}\left(k - \frac{1}{R_\mathrm{e}}\right) - U_\mathrm{gs2}k \\ &+ f(U_\mathrm{gs1})\left(\frac{1}{pR_1} - 1\right) - f(U_\mathrm{gs2}) - \frac{U_\mathrm{o}}{pR_\mathrm{c1}R_1} \\ 0 &= U_\mathrm{in}k - U_\mathrm{gs1}k + U_\mathrm{gs2}k - \frac{f(U_\mathrm{gs1})}{pR_1} + \frac{U_\mathrm{o}}{pR_\mathrm{c1}R_1}\end{aligned} \tag{9}$$

where the constants p and k are

$$p = \frac{1}{R_\mathrm{c1}} + \frac{1}{R_1} \tag{10}$$

$$k = \frac{1}{pR_1^2} - \frac{1}{R_1} - \frac{1}{R_2} \tag{11}$$

The system of equations is solved using Newton-Raphson method where the range of U_gs1 is defined. To find the fold in the state space we need to choose a proper coordinate system. Since U_in is fixed, this state cannot jump. This implies that we need to look at the $U_\mathrm{in} - U_\mathrm{out2}$ curve for a fold. Figure 4 indeed shows a fold and as expected, there are multiple

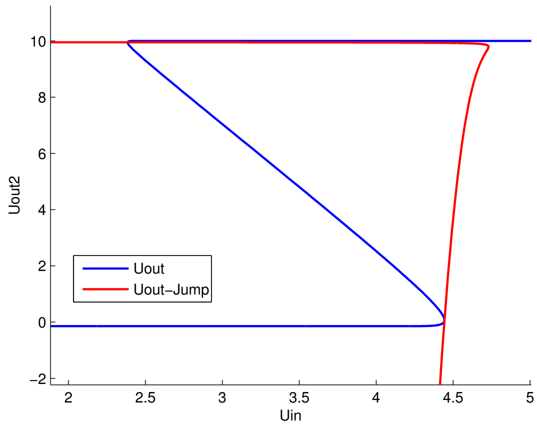

Fig. 4. Output vs. Input – Schmitt Trigger.

outputs for the same input indicating singularity. To calculate the point where the output transition occurs, we calculate the jump points using the method as stated in Eq. (3). This gives us

$$\begin{aligned} &k\left((k-1)+f'(U_{\mathrm{gs1}})\left(\frac{1}{pR_1}-1\right)\right)\\ &-\left(k+f'(U_{\mathrm{gs2}})\right)\left(k+\frac{f'(U_{\mathrm{gs1}})}{pR_1}\right)=0 \end{aligned} \tag{12}$$

To solve this equation we assume that U_{gs1} varies between two predefined values and find U_{gs2}. The intersections of the solution set of Eq. (12) and the state space are defined as the jump points. The jump points of the output are shown in Fig. 4 as the intersection of both curves.

5 Example 2: Flip Flop circuit

The flip flop circuit is analyzed similar to the previous case. This circuit is analytically similar to the Schmitt Trigger, hence the results should be similar to the ones obtained there. The following are the design parameters of the circuit: $U_{\mathrm{o}}=9\,\mathrm{V}$, $V_{\mathrm{T}}=1.6\,\mathrm{V}$, $R_{\mathrm{c1}}=10\,\Omega$, $R_{\mathrm{c2}}=10\,\Omega$, $R_{\mathrm{b1}}=10\,\mathrm{k\Omega}$, $R_{\mathrm{b2}}=10\,\mathrm{k\Omega}$, $R_x=10\,\mathrm{k\Omega}$, $R_y=10\,\mathrm{k\Omega}$ and $R_v=5\,\mathrm{k\Omega}$. The equations governing the circuit are

$$\begin{aligned} 0&=\frac{U_0}{qR_{\mathrm{b1}}R_{\mathrm{c2}}}-\left(k-\frac{1}{qR_{\mathrm{b1}}^2}\right)U_{\mathrm{gs1}}-\frac{f(U_{\mathrm{gs2}})}{qR_{\mathrm{b1}}}+\frac{U_{\mathrm{in}}}{R_v}\\ 0&=\frac{U_0}{pR_{\mathrm{c1}}R_{\mathrm{b2}}}+\left(\frac{1}{pR_{\mathrm{b2}}^2}-\frac{1}{R_{\mathrm{b2}}}-\frac{1}{R_x}\right)U_{\mathrm{gs2}}-\frac{f(U_{\mathrm{gs1}})}{pR_{\mathrm{b2}}} \end{aligned} \tag{13}$$

where the constants k, p, q are

$$k=\frac{1}{R_{\mathrm{b1}}}+\frac{1}{R_v}+\frac{1}{R_y} \tag{14}$$

$$p=\frac{1}{R_{\mathrm{c1}}}+\frac{1}{R_{\mathrm{b2}}} \tag{15}$$

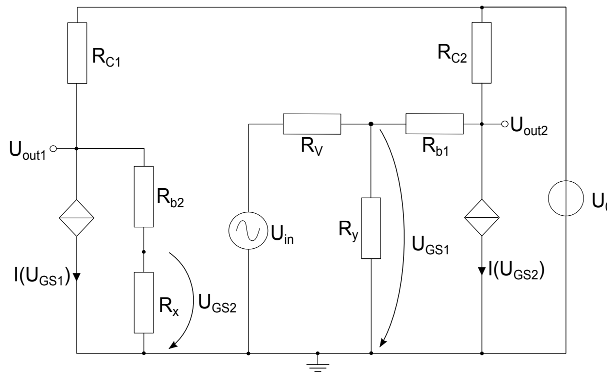

Fig. 5. Flip Flop Circuit.

$$q=\frac{1}{R_{\mathrm{c2}}}+\frac{1}{R_{\mathrm{b1}}}. \tag{16}$$

U_{in} is the independent input voltage, U_{out2} is the output and U_{gs1}, U_{gs2} are the gate source voltages of the MOS. The state space and the jump points are obtained by declaring U_{gs1} between two predefined values and solving for U_{gs2} for that corresponding value of U_{gs1}. The determinant criterion here turns out to be

$$\begin{aligned} &\left(\frac{1}{R_{\mathrm{b1}}^2q}-k\right)\left(\frac{1}{pR_{\mathrm{b2}}^2}-\frac{1}{R_{\mathrm{b2}}}-\frac{1}{R_x}\right)\\ &\quad-\frac{f'(U_{\mathrm{gs1}})f'(U_{\mathrm{gs2}})}{pqR_{\mathrm{b1}}R_{\mathrm{b2}}}=0 \end{aligned} \tag{17}$$

The jump points of the output are shown in Fig. 6 as the intersection of both curves.

6 Example 3: multivibrator

In the earlier sections the systems of equations were only algebraic ones. Here, for the multivibrator, we get a semi explicit DAE system. The device parameters chosen for this circuit are: $U_{\mathrm{o}}=5\,\mathrm{V}$, $V_{\mathrm{T}}=1.6\,\mathrm{V}$, $R_1=5\,\mathrm{k\Omega}$, $R_2=100\,\mathrm{k\Omega}$, $C=33\,\mathrm{nF}$, $I_{\mathrm{o}}=0.26\,\mathrm{mA}$. The equations governing this circuit are:

$$\begin{aligned} 0=&\frac{U_0R_1-U_{\mathrm{gs1}}\left(R_1+\frac{R_2}{2}\right)+\frac{U_{\mathrm{gs2}}R_2}{2}}{R_1(R_1+R_2)}\\ &+\frac{I_0R_1R_2-\frac{U_c(R_1+R_2)}{2}}{R_1(R_1+R_2)}-f(U_{\mathrm{gs2}}) \end{aligned}$$

$$\begin{aligned} 0=&\frac{U_0R_1+\frac{U_{\mathrm{gs1}}R_2}{2}-U_{\mathrm{gs2}}\left(R_1+\frac{R_2}{2}\right)}{R_1(R_1+R_2)}\\ &+\frac{\frac{U_{\mathrm{c}}(R_1+R_2)}{2}+I_0R_1R_2}{R_1(R_1+R_2)}-f(U_{\mathrm{gs1}}) \end{aligned}$$

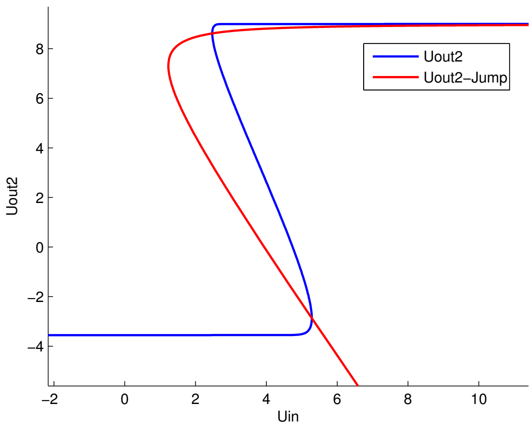

Fig. 6. Output vs. Input – Flip Flop.

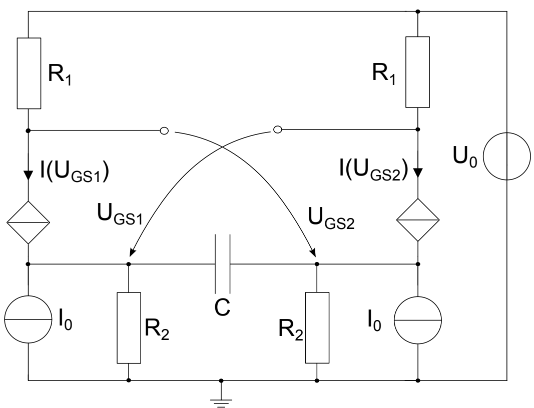

Fig. 7. Multivibrator Circuit Diagram.

$$\dot{U}_{\mathrm{c}} = -\frac{\left(\frac{U_{\mathrm{c}}}{2} - R_2 f(U_{\mathrm{gs1}}) + R_2 f(U_{\mathrm{gs2}})\right)}{C R_2}$$

$$-\frac{\left(\frac{R_2 U_{\mathrm{gs1}}}{2} - \frac{R_2 U_{\mathrm{gs2}}}{2} + \frac{R_2 U_{\mathrm{c}}}{2}\right)}{C R_1 R_2} \tag{18}$$

The above equations can be written in a matrix form as

$$\begin{pmatrix} 0 \\ 0 \\ \dot{U}_{\mathrm{c}} \end{pmatrix} = \boldsymbol{h}(U_{\mathrm{gs1}}, U_{\mathrm{gs2}}, U_{\mathrm{c}}) \tag{19}$$

The state space of the circuit is given by the intersection of the surfaces S_1 and S_2, where S_1 is the solution set of $h_1(U_{\mathrm{gs1}}, U_{\mathrm{gs2}}, U_{\mathrm{c}}) = 0$ and S_2 is the solution set of $h_2(U_{\mathrm{gs1}}, U_{\mathrm{gs2}}, U_{\mathrm{c}}) = 0$. Figure 8 shows the intersection of the two surfaces. The intersection curve (in blue) is the state space of the circuit. The state space has to be plotted in a coordinate system, where one of the quantity does not jump whereas the other two show jump behavior. Hence the state

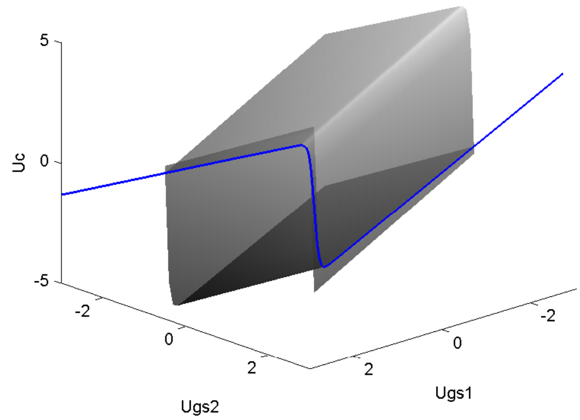

Fig. 8. State space as intersection of S_1 and S_2.

space was plotted in $U_{\mathrm{gs1}} - U_{\mathrm{gs2}} - U_{\mathrm{c}}$ coordinate system. The determinant criterion for this circuit is given as

$$\frac{\left(R_1 + \frac{R_2}{2}\right)^2}{R_1(R_1 + R_2)} - \left(\frac{R_2}{2R_1(R_1 + R_2)} - f'(U_{\mathrm{gs1}})\right) \cdot \\ \cdot \left(\frac{R_2}{2R_1(R_1 + R_2)} - f'(U_{\mathrm{gs2}})\right) = 0 \tag{20}$$

Upon solving this with Newton-Raphson method we get the jump points as shown in Fig. 9. The jump points are shown in the $U_{\mathrm{gs1}} - U_{\mathrm{gs2}}$ coordinate system as the intersection of both curves. For verifying our results we regularized the system of equations by adding regularization capacitances parallel to U_{gs1} and U_{gs2}. The transient behavior of this regularized circuit can be seen in Fig. 10 (red line). We can see that the fast transition occurs in the U_{gs1} and U_{gs2} space, where the capacitance potential U_{c} is hold mostly constant.

7 Conclusions

The simulation of electronic circuits that contain a fold in their state space with common circuit simulators like SPICE sometimes gives errors due to time constant problems. The analysis of these circuits require regularization, which is achieved by adding capacitors and inductors at appropriate nodes. If the regularization is not done in accordance with Tikhonov's Theorem, the transient solutions will not be reliable. With our approach, regularization is no longer necessary, as it is possible to detect whether the manifold of the circuit's state space has a fold beforehand. The jump points, therefore help us to identify the points of transition easily. We have shown numerical results of applying the geometric concepts to three MOS circuits. Therefore, the MOS drain current was modelled using the EKV equation for robust results.

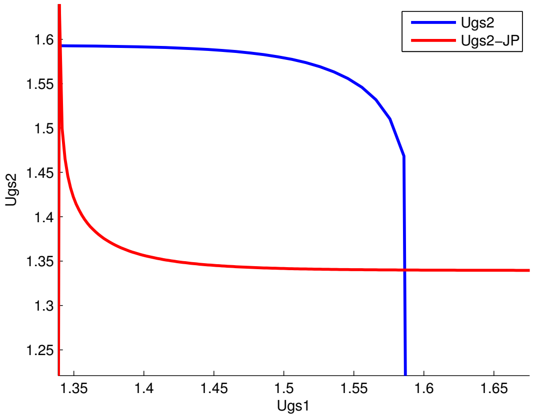

Fig. 9. Jump points in the $U_{\mathrm{gs1}} - U_{\mathrm{gs2}}$ coordinate system.

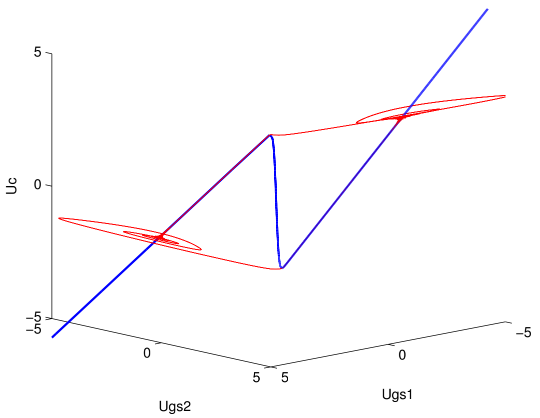

Fig. 10. Transient solution (red) of the regularized circuit in the $U_{\mathrm{gs1}} - U\mathrm{gs2} - U\mathrm{c}$ coordinate system; state space of non-regularized circuit (blue).

Acknowledgements. The authors would like to thank the German Research Foundation (DFG) and the German Academic Exchange Service (DAAD) for the financial support.

References

Chua, L.: Dynamic nonlinear networks: State-of-the-art, IEEE T. Circuits Syst., CAS-27, 1059–1087, 1980.

Desoer, C. and Wu, F.: Trajectories of nonlinear RLC networks: A geometric approach, IEEE T. Circuit Syst., 19, 562–571, 1972.

Enz, C. C., Krummenacher, F., and Vittoz, E. A.: An analytical MOS transistor model valid in all regions of operation and dedicated to low-voltage and low-current applications, Analog Integr. Circuits Signal Process., 8, 83–114, 1995.

Ichiraku, S.: Connecting Electrical Circuits: Transversality and Well-Posedness, Yokohama Mathematical Journal, 27, 111–126, 1979.

Ihrig, E.: The Regularization of Nonlinear Electrical Circuits, P. Am. Math. Soc., 47, 179–183, 1975.

Mathis, W.: Geometric theory of nonlinear dynamical networks, in: Computer Aided Systems Theory EUROCAST – ’91, edited by: Pichler, F. and Díaz, R., vol. 585 of *Lecture Notes in Computer Science*, 52–65, Springer Berlin/Heidelberg, 1992.

Nielsen, R. O. and Willson Jr., A. N.: A fundamental result concerning the topology of transistor circuits with multiple equilibria, Proc. of the IEEE, 68, 196–208, 1980.

Sandberg, I. W. and Shichman, H.: Numerical integration of systems of stiff nonlinear differential equations, Bell Syst. Tech. J., 47, 511–527, 1968.

Sastry, S. and Desoer, C.: Jump behavior of circuits and systems, IEEE T. Circuits Syst., 28, 1109–1124, doi:10.1109/TCS.1981.1084943, 1981.

Smale, S.: On the mathematical foundation of electrical circuit theory, J. Differ. Geom., 7, 193–210, 1972.

Tchizawa, K.: An Analysis of Nonlinear Systems with Respect to Jump, Yokohama Mathematical Journal, 32, 203–214, 1984.

Thiessen, T. and Mathis: Geometric Dynamics of Nonlinear Circuits and Jump Effects, International Journal of Computations & Mathematics in Electrical & Electronic Engineering (Compel 2011), 30, 1307–1318, 2011.

Thiessen, T., Gutschke, M., Blanke, P., Mathis, W., and Wolter, F.-E.: A Numerical Approach for Nonlinear Dynamical Circuits with Jumps, in: 20th European Conference on Circuit Theory and Design (ECCTD 2011), 2011.

Thiessen, T., Plönnigs, S., and Mathis, W.: Transient Solution of Fast Switching Systems without Regularization, in: IEEE 55th International Midwest Symposium on Circuits and Systems (MWSCAS 2012), 578–581, 2012.

Tikhonov, A. N., Vasil’eva, A. B., and Sveshnikov, A. G.: Differential Equations, Springer-Verlag, Berlin-Heidelberg-New York-Tokyo, 1985.